Clinical Biomechanics 99 (2022) 105766

Contents lists available at ScienceDirect

Clinical Biomechanics

journal homepage: www.elsevier.com/locate/clinbiomech

Regulation of whole-body and segmental angular momentum in persons with Parkinson's disease on an irregular surface

Nicholas G. Gomez [a], K. Bo Foreman [b], MaryEllen Hunt [a], Andrew S. Merryweather [a,*]

[a] Department of Mechanical Engineering, University of Utah, Salt Lake City, UT, USA
[b] Department of Physical Therapy, University of Utah, Salt Lake City, UT, USA

ARTICLE INFO

Keywords:
Dynamic balance
Falls
Gait
Parkinson's disease
Biomechanics
Older adults

ABSTRACT

Background: Persons with Parkinson's disease have impaired motor control that increases their chance of falling when walking, especially on difficult terrains. This study investigated how persons with Parkinson's disease regulate their dynamic balance on a regular and an irregular surface.

Methods: Nine participants with Parkinson's disease and nine healthy, age-matched control participants ambulated on both a regular and an irregular surface. Whole-body and segmental angular momenta were calculated using three-dimensional motion capture data. Major modes of variability between health groups on the two surfaces were investigated using principal component analysis, while differences within each health group between surfaces was investigated using statistical parametric mapping *t*-tests.

Findings: Between groups, the Parkinson participants had greater sagittal, frontal, and transverse whole-body angular momentum on both surfaces, primarily following heel-strike, and the magnitude difference on the irregular surface was greater than on the regular surface. The greatest between group segmental differences on the irregular compared to the regular surface were the legs in the sagittal plane and the head/trunk/pelvis in the transverse plane, with the Parkinson group having greater magnitudes. The within-group comparison found the Parkinson participants had poorer regulation of whole-body angular momentum in the sagittal plane, while the healthy participants showed no consistent differences between surfaces.

Interpretation: On an irregular surface, persons with Parkinson's disease exhibit poor control of dynamic balance in the frontal and sagittal planes. These results emphasize the need for weight transfer techniques and training in both the sagittal and frontal planes to maximize balance and reduce fall risk.

1. Introduction

Whole-body angular momentum (WBAM) in relation to the body's center of mass (COM) is highly regulated in overground walking (Robert et al., 2009). Additionally, WBAM as well as the segmental contributions to this metric, have been found to be sensitive to alternative conditions apart from level, overground walking. For example, while negotiating 90-degree turns, healthy individuals were found to have significant increases in segmental angular momentum during the turning procedure (Nolasco et al., 2019). Further, during stair ascent and descent (Silverman et al., 2014) and slope walking (Silverman et al., 2012), it was found that participants actively counteracted sagittal angular momentum to minimize potential trips or falls.

Regulation of WBAM has also been shown to be sensitive to age. Older individuals exhibit greater increases in sagittal whole-body and segmental angular momentum during step initiation (Begue et al., 2019), stepping (Begue et al., 2021), and level walking (Vistamehr et al., 2021). Because of these observed changes and the inability to regulate WBAM during "normal" ambulation, it can be inferred that an understanding of the further effect of a perturbation, or even a destabilizing surface, is paramount to reducing potential fall risk in the older population (Neptune and Vistamehr, 2019).

How the above findings extend to persons with a neurological impairment, such as Parkinson's disease (PD), is relatively unknown. A recent investigation found that in stair descent, persons with PD increased their sagittal and transverse WBAM during stair descent compared to a healthy control population (Li and Fey, 2021). However, the generalizability of these findings is limited due to small sample size ($N = 5$). Research has also shown that persons with PD increase the root-mean-square of their trunk acceleration and alter their lower-limb

* Corresponding author at: Mechanical Engineering, University of Utah, 1495 E 100 S, Salt Lake City, UT 84112, USA.
E-mail addresses: nicholas.gomez@utah.edu (N.G. Gomez), bo.foreman@hsc.utah.edu (K.B. Foreman), a.merryweather@utah.edu (A.S. Merryweather).

https://doi.org/10.1016/j.clinbiomech.2022.105766
Received 9 March 2022; Accepted 12 September 2022
Available online 15 September 2022

kinematics and kinetics on irregular terrains (Xu et al., 2018). Lower limb kinematics changes have been observed, as well, when negotiating surface transitions (Gomez et al., 2020).

Considering the aforementioned effects of walking conditions and age, it is important to investigate how known gait and postural impairments characteristic of PD potentially impact regulation of WBAM (Massano and Bhatia, 2012). Specifically, data regarding an impaired regulation of this parameter is necessary because angular momentum that is not cancelled can lead to the COM exceeding the base of support and thus, lead to a fall (Chiovetto et al., 2018). Therefore, we sought to determine how persons with PD regulate their WBAM when ambulating on both a regular surface and a destabilizing irregular surface compared to healthy, age-matched controls (HC). Our first objective was to identify how the segments of the body contribute to regulation of WBAM. We hypothesized that the major modes of variability in the regulation of WBAM between health groups would be similar for the regular and irregular surfaces, but the segmental contributions would be different. Our second objective was to investigate differences within each group between surfaces to identify specific aspects of the gait cycle (GC) that were impacted by the change in surface condition. For the second objective, we hypothesized that within each health group, there would only be significant differences at the segmental level when comparing the regular to the irregular surface.

2. Methods

2.1. Participants

Participants were recruited as a convenience sample from the University of Utah and the Rehabilitation and Wellness clinic hosted by the University of Utah's Physical Therapy Department. This study was approved by the University of Utah's Internal Review Board (IRB Approval #52667). Participants with PD were included if they were $\geq$ 50 years old, had a Hoehn & Yahr score between two and three, did not have an injury or other illness that prevented participation in the study, and did not have a deep brain stimulator implanted. The healthy controls were included if they were $\geq$ 50 years old, were not physically impaired, and had no injury or other illness that prevented participation in the study. As a result of our recruitment, nine persons with PD comprised the experimental group and consisted of five males and four females with an age of 67.7 $\pm$ 7.1 years, a height of 1.66 $\pm$ 0.16 m, a mass of 81.0 $\pm$ 20.6 kg, walking speeds of 0.78 $\pm$ 0.26 m/s and 0.91 $\pm$ 0.24 m/s on the irregular and regular surfaces, respectively, a Unified Parkinson's Disease Rating Scale score of 36.1 $\pm$ 11.8, and a Hoehn & Yahr score of 2.39 $\pm$ 0.31. The control group contained nine healthy, age-matched controls (HC). There were six males and three females aged 67.7 $\pm$ 8.0 years, with a height of 1.69 $\pm$ 0.05 m, a mass of 74.5 $\pm$ 5.6 kg, and walking speeds of 1.12 $\pm$ 0.16 m/s and 1.18 $\pm$ 0.17 m/s on the irregular and regular surfaces, respectively. All participants provided informed consent prior to participation in the study protocol.

2.2. Study protocol

Participants wore tight-fitting clothes onto which 76 reflective markers were placed according to a modified Helen Hayes marker set. Participants also wore a safety harness that was connected to a low-friction overhead rail. Participants with PD took their dopaminergic medication within three hours of being evaluated and verbally expressed feeling in an "ON" medication state. The study environment consisted of a custom 7.3 m long by 0.76 m wide walkway that was made of oriented-strand board (OSB). The participants completed trials on two different surface conditions: 1) regular: exposed OSB and 2) irregular: OSB walkway covered in faux-rock panels (Model R3-RV-PN-MT, Regency River Rock, http://FauxPanels.com) (Fig. 1). Three-dimensional marker trajectories were captured at 100 Hz with twenty-four cameras (NaturalPoint, Corvallis, OR, USA) and later processed in Visual3D (C-motion, Germantown, MD, USA) using a 4th order low-pass Butterworth filter at a cutoff frequency of 6 Hz. Cutoff frequency was determined by visual inspection and residual analysis (Winter, 1990). Prior to data collection, participants ambulated on both surface conditions until they expressed verbal familiarity and comfort walking on the two surfaces. Once data collection began, participants ambulated back and forth at least three times on each surface.

2.3. Study outcomes

Successful trials were defined as those that had all markers present for the full gait cycle (GC) that started closest to the midpoint of the walkway to ensure that participants were at steady-state gait. From the successful trials, a single, representative trial was selected from each participant to analyze. GCs were established using heel strikes identified by the kinematic Event TPOR Signal in Visual 3D (Stanhope et al., 1990) and verified with manual inspection. The main outcomes of interest in this study were WBAM and the contributions to this metric by the major segment groups of the body: arms, legs, and a head/trunk/pelvis (HTP) segment. A 13-segment model in Visual3D (head, torso, pelvis, arms, forearms, thighs, shanks, and feet) was used to calculate the center of mass (COM) location and velocity of each segment as well as the whole

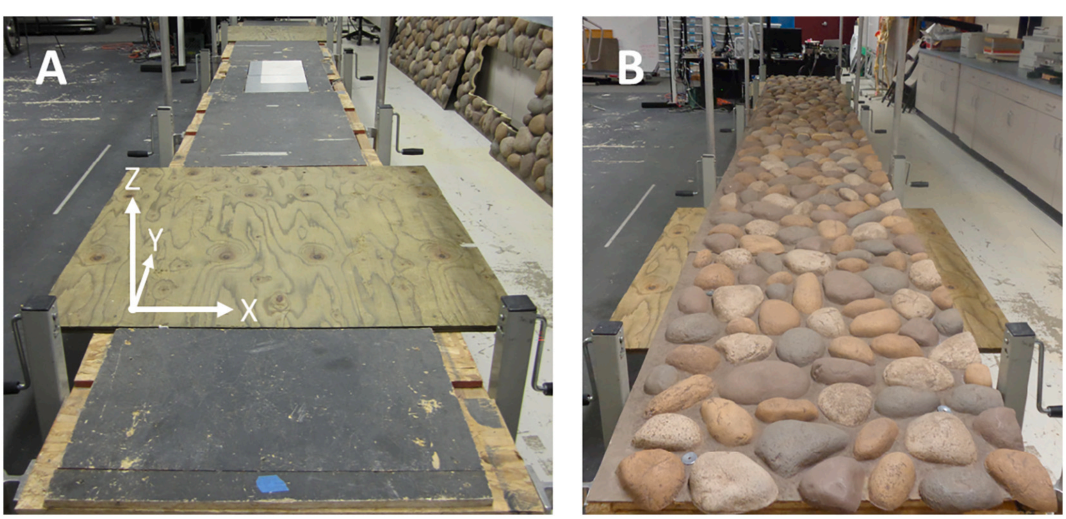

Fig. 1. Picture of regular surface (A) and irregular surface (B). Coordinate orientation utilized to define positive angular momentum depicted in (A) and follows the right-hand rule. Z is the axis for the transverse plane, X is the axis for the sagittal plane, and Y is the axis for the frontal plane.

body as determined by the summation of segmental contributions about the body's COM. The whole-body angular momentum, WBAM, was defined using Eq. 1 below:

$$WBAM = \sum_{i=1}^{n} [\mathbf{I}_i \boldsymbol{\omega}_i + \mathbf{r}_{COM} \times m_i \mathbf{v}_i] \quad (1)$$

Here, $\mathbf{I}_i$ and $\boldsymbol{\omega}_i$ are the moment of inertia and angular velocity of the i-th segment, respectively, $\mathbf{r}_{COM}$ is the distance from the body COM to the COM of the i-th segment, m_i is the mass of the i-th segment, and $\mathbf{v}_i$ is the translational velocity of the i-th segment with respect to the body center of mass. Segment masses were calculated as a function of each participant's body mass and the inertial properties were defined using the marker data and assumed representative geometries (Hanavan Jr., 1964). Positive sagittal momentum was defined as rotating backward, positive frontal momentum was defined as leaning right, and positive transverse momentum was defined as turning toward the left leg (Fig. 1). Time-series data of the angular momentum for the whole body and each segment group about each axis were normalized to 101 data points as well as participant height, mass, and average walking velocity from beginning to end of the representative trial to make the final data unitless. Following normalization, data were smoothed with a gaussian filter using a window width of three data points.

2.4. Statistical analyses

Major modes of variability between the health groups on the regular and the irregular surface were identified using principal component (PC) analysis. PC analysis has been applied to time-series biomechanics data using a variety of different approaches (Bennett et al., 2010; Herr and Popovic, 2008; Chiovetto et al., 2018; Reid et al., 2010; Chester and Wrigley, 2008; Monaghan et al., 2021; Tsuchida et al., 2022). In the present study, the 12 waveforms (angular momentum for the whole body, arms, legs, and head/trunk/pelvis segments about the x, y, and z axes) were grouped together resulting in 12 matrices with dimension 18 × 101 (number of total participants × number of data points). PC analysis was applied to the covariance matrix of the 12 matrices to determine the PC coefficients, which indicate the amount of variability each PC explains, and the PC scores (*Z*-scores), which indicate how the shape of a group's representative waveform differs from the mean of both health groups combined. Only the PCs that summed to explain 90% or more of the variability for each matrix were kept for analysis (Jackson, 1991). Z-scores for the retained PCs for each health group were compared using non-parametric, two-sample *t*-tests since Z-scores were not normally distributed. The alpha for significance was adjusted for multiple comparisons using the Benjamini-Hochberg method (Benjamini and Hochberg, 1995) which resulted in an adjusted alpha of $P < 0.0091$.

The normalized whole-body and segment group angular momentum about each axis were compared between surface conditions (regular and irregular) for each health group separately using non-parametric, two-tailed statistical parametric mapping (npSPM) paired *t*-tests with an alpha level of 0.05 (Pataky, 2012) since data were not normally distributed. Both the npSPM and PC analyses were performed in MATLAB (R2020a; MathWorks, Natick, MA.)

3. Results

3.1. Between health group comparisons for the regular and the irregular surfaces

The two-sample t-tests identified 10 PC's that were significantly different between health groups on the regular surface and 9 PC's that were significantly different on the irregular surface (Table 1). Biomechanical interpretation of the significant PC's was accomplished using the method of visually inspecting the loading vector as well as the angular momentum curves. The reconstructed angular momentum curves were generated from the product of the 5th and 95th percentile *Z*-scores and the loading vector, which were added to the raw mean of the angular momentum waveforms, respectively (Figs. 2,3) (Brandon et al., 2013).

Table 1
Description of principal components that were significantly different between PD group and HC group for the regular and irregular surfaces.

Outcome	PC	Variance Explained(%)	Mean (SD) *Z*-Scores		*P*-Values
Regular Surface			PD	HC	
WBAM Sagittal	1	68.5	−0.026 (0.043)	0.026 (0.027)	0.008
WBAM Frontal	1	69.3	−0.025 (0.025)	0.025 (0.009)	<0.001
WBAM Transverse	1	79.5	−0.012 (0.016)	0.012 (0.008)	0.003
Arms Sagittal	1	26.7	−0.001 (0.001)	0.001 (0.001)	<0.001
Arms Frontal	1	46.0	0.002 (0.002)	−0.002 (0.002)	0.005
Arms Transverse	1	81.4	0.008 (0.007)	−0.008 (0.006)	<0.001
Legs Frontal	1	60.9	−0.014 (0.012)	0.014 (0.005)	<0.001
Head/Trunk/ Pelvis Sagittal	1	34.0	−0.007 (0.010)	0.007 (0.006)	0.002
Head/Trunk/ Pelvis Frontal	1	66.5	−0.010 (0.013)	0.010 (0.007)	0.002
Head/Trunk/ Pelvis Transverse	1	36.7	−0.002 (0.002)	0.002 (0.002)	<0.001
Irregular Surface					
WBAM Sagittal	1	75.6	−0.052 (0.087)	0.052 (0.032)	0.007
WBAM Frontal	1	65.9	−0.039 (0.041)	0.039 (0.017)	<0.001
WBAM Transverse	1	64.6	0.012 (0.018)	−0.012 (0.010)	0.004
Arms Frontal	1	65.6	0.003 (0.005)	−0.003 (0.003)	0.006
Arms Transverse	1	75.0	0.007 (0.007)	−0.007 (0.010)	0.003
Legs Sagittal	1	75.3	−0.035 (0.061)	0.035 (0.028)	0.009
Legs Frontal	1	60.4	−0.022 (0.021)	0.022 (0.007)	<0.001
Head/Trunk/ Pelvis Sagittal	1	56.6	−0.016 (0.024)	0.016 (0.007)	0.004
Head/Trunk/ Pelvis Frontal	1	57.9	−0.015 (0.016)	0.015 (0.011)	<0.001

There were 8 PC's that were consistent between the surfaces both in terms of significance and mode of variability captured. In the sagittal plane, PC1 was a magnitude and phase shift operator for the WBAM (Figs. 2A,3A) and though the HTP segment followed the same pattern as the WBAM, the magnitude was not well captured, making this PC primarily a phase shift operator for this segment (Figs. 2H,3H). Significant differences in the frontal plane were found in PC1 of all segments: WBAM (Fig. 2B,3B), arms (Fig. 2E,3D), legs (Fig. 2G,3G), and HTP (Fig. 2I,3I). PC1 for the arms and HTP were magnitude operators while PC1 for the WBAM and legs captured both magnitude and phase shift. The lack of phase shift in the arms and HTP indicate that the legs were the primary contributor to the phase shift observed in the WBAM. In the transverse plane, PC1 was significantly different between groups for the WBAM (Fig. 3C) and the arms (Fig. 3E), both of which were magnitude operators. Though these modes of variability were consistent for both surfaces, the magnitudes were always greater on the irregular surface (Fig. 3) compared to the regular surface (Fig. 2).

Variables that were not consistent between the two health groups were PC1 for sagittal arm angular momentum (Fig. 2D), PC1 for sagittal leg angular momentum (Fig. 3F), and PC1 for transverse HTP angular

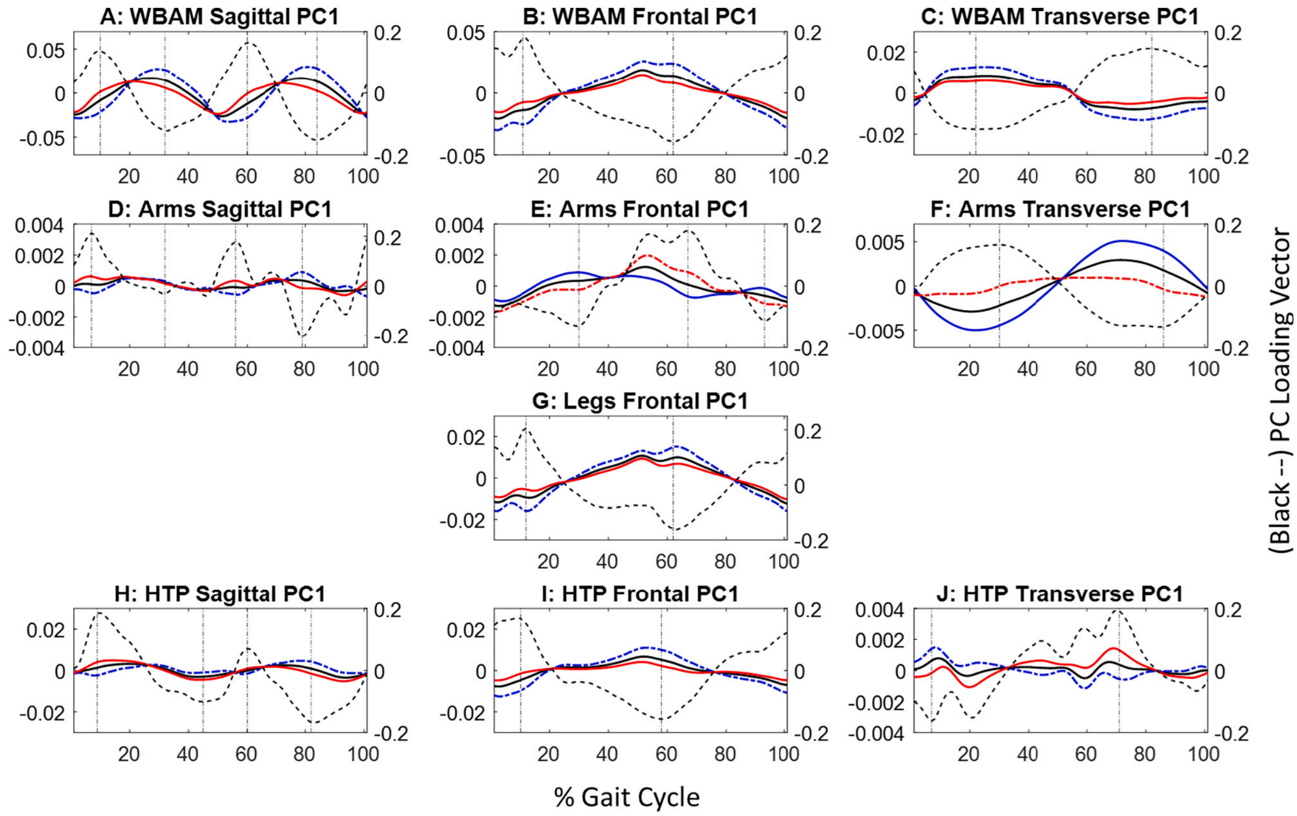

Fig. 2. Graphical representation of reconstructed angular momentum data (unitless) for the regular surface using PC1 for each metric. Each tile presents the mean of the original data (solid black line), the reconstructed data using the 5th (blue) and 95th (red) percentile Z-scores, and the loading vector (dashed black line). Data were reconstructed using the product of the Z-score with the loading vector, which was then added to the mean. Note that since the 5th and 95th percentile values did not always come from the same health group, the dashed colored line indicates the PD group, and the solid-colored line indicates the HC group. Vertical lines identify for clarity where the loading vector reaches its highest magnitudes. (For interpretation of the references to colour in this figure legend, the reader is referred to the web version of this article.)

momentum (Fig. 2J). These were all magnitude operators, so they indicate when the health groups became more or less similar to the PD group going from the regular surface to the irregular surface. The HC group increased their sagittal arm angular momentum on the irregular surface, which made the contribution from that segment the same as exhibited by the PD group. The PD group increased the sagittal contribution of their legs as well as exhibited a phase shift when walking on the irregular surface. On the regular surface, the PD group had greater magnitude of transverse HTP angular momentum than the HC group, but that difference disappeared on the irregular surface.

3.2. *Differences between the regular and irregular surfaces for each health group, independently*

The PD group exhibited most of their differences between the regular and irregular surfaces in the sagittal plane. Their whole-body angular momentum showed consistent increases during single limb support phase, which is between 12 and 50% of the gait cycle, and during second double limb support, the latter being between 50 and 62% of the cycle when weight transfer began to the trailing limb (Fig. 4A) (Sutherland et al., 1994). The arms (Fig. 5A), legs (Fig. 5B), and HTP segments (Fig. 4B) all contributed to the sagittal forward acceleration during weight transfer (i.e. 50–62% GC) and deceleration during initial swing phase (i.e. 12–50% GC) as identified by the whole-body summation. Apart from the differences in the sagittal plane, the only other notable differences for the PD group between the two surface conditions were the legs, where they decreased the angular momentum in the frontal plane during single limb support (i.e. 12–50% GC) and increased transverse angular momentum during initial swing (i.e. 62–75% GC) on the irregular surface compared to the regular surface.

The HC group showed similar adjustments to their sagittal angular momentum between surfaces but not nearly to the same degree as the PD group. Minor deviations were observed in the whole-body angular momentum during single limb support (i.e. 12–50% GC) where the HC group also had greater forward angular acceleration on the irregular surface (Fig. 4A). The legs and the HTP segments were the primary contributors to the increased forward angular momentum (Figs. 5B, 4B) during initial single limb support. The HC group also increased their transverse whole-body angular momentum (Fig. 4E) during second double limb support (i.e. 50–62% GC) on the irregular surfaces and the segments that contributed to this increase were the arms (Fig. 5E) and HTP (Fig. 4F).

4. Discussion

This study first investigated how each health group regulated their WBAM on both a regular and an irregular surface and how the segments of the body contributed to that regulation. We hypothesized that since WBAM is generally highly regulated (Robert et al., 2009), the major modes of variability in the regulation of WBAM between health groups would be similar for the regular and irregular surfaces. We further hypothesized that the segmental contributions would be different due to the known motor control deficits in persons with PD (Xu et al., 2018). These hypotheses were mostly supported. The PC analysis identified that the PD group had significantly different regulation of WBAM compared to the HC group on both surfaces. At the whole-body level, the primary difference between health groups was just the magnitude of angular momentum in each anatomical plane. However, in the sagittal and

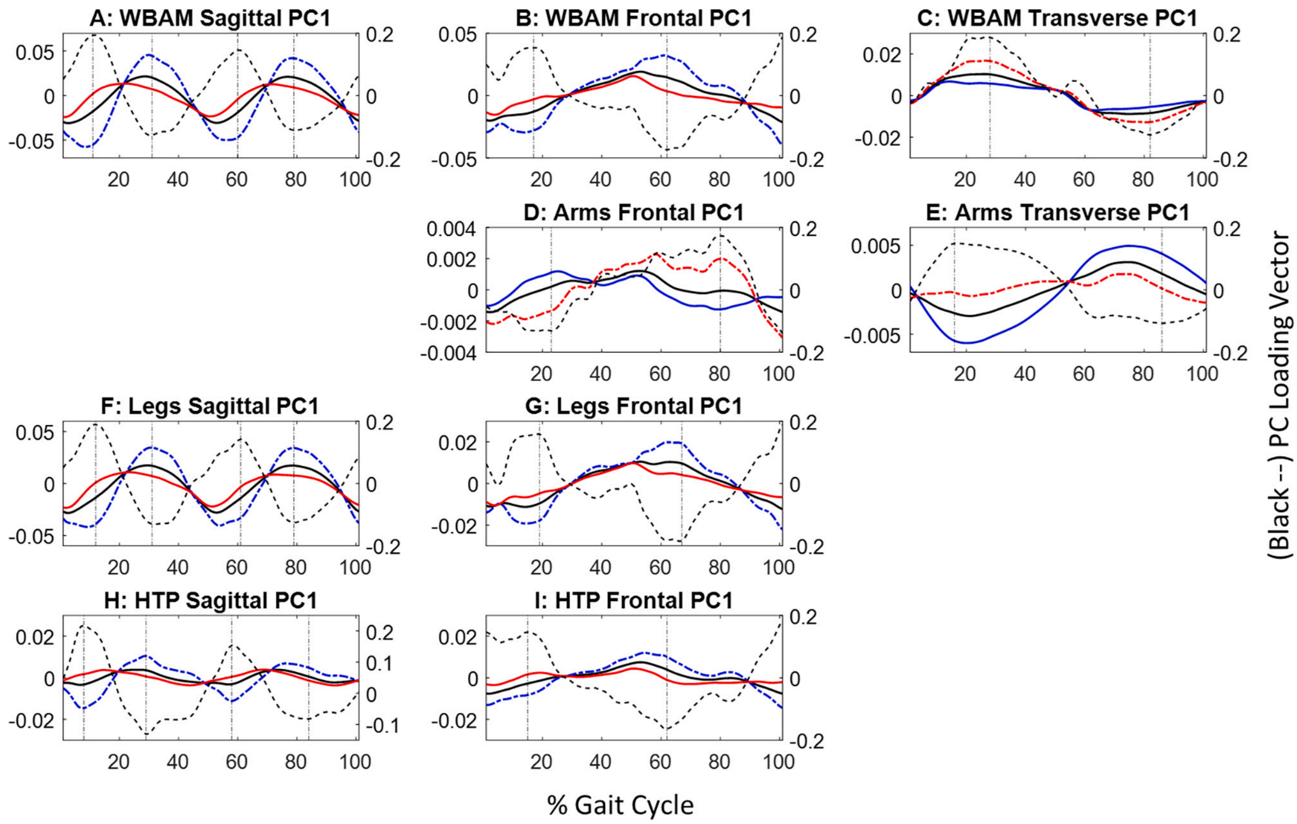

Fig. 3. Graphical representation of reconstructed angular momentum data (unitless) for the irregular surface using PC1 for each metric. Each tile presents the mean of the original data (solid black line), the reconstructed data using the 5th (blue) and 95th (red) percentile Z-scores, and the loading vector (dashed black line). Data were reconstructed using the product of the Z-score with the loading vector, which was then added to the mean. Since the 5th and 95th percentile values did not always come from the same health group, the dashed colored line indicates the PD group, and the solid-colored line indicates the HC group. Vertical lines identify for clarity where the loading vector reaches its highest magnitudes. (For interpretation of the references to colour in this figure legend, the reader is referred to the web version of this article.)

transverse planes, the segmental contribution to the observed increase at the whole-body level was not the result of all segments increasing proportionally. In the sagittal plane, the two health groups had similar leg angular momentum and the primary differences were found in the arms and HTP segments, where the PD group had greater magnitude. When walking on the irregular surface, the HC group adapted by increasing the contribution of their arms to the point it matched the PD group. The PD group on the other hand greatly increased the contribution from their HTP and legs segments, which created the more pronounced magnitude and phase shift difference observed in the sagittal WBAM (Fig. 3A).

These differences in the sagittal plane have implications in terms of fall risk. The PD group experienced rapid forward angular momentum during stance phase following heel strike that they had to then cancel out during swing phase. These increases potentially were the result of increased leg movements often exhibited by persons with PD to increase their minimum-toe-clearance (Gomez et al., 2020). The significant increase compared to the HC group indicates that the PD group may have been overcompensating with their lower limbs. Significant differences were found on both surfaces between groups in the frontal plane. The main difference observed was a magnitude increase in the PD group on the irregular surface. This meant that the PD group experienced a greater lateral shift onto their leading limb that would lead their center of pressure to travel closer to the lateral edge of their base of support (Chiovetto et al., 2018; Herr and Popovic, 2008). Poor regulation of frontal angular momentum has been shown to have implications regarding severity of a slip should one occur (Nazifi et al., 2020). During weight transfer, the hip extensors and ankle dorsiflexors are most active in the sagittal plane (Neptune and McGowan, 2011), and in the frontal plane, the leg abductors are most active (Neptune and McGowan, 2016). There were declines in both planes of motion on the irregular surface in the PD group so all these muscles would benefit from strength and coordination training to improve regulation of dynamic balance to reduce risk of falling, especially on the irregular surface.

There were also segmental differences in regulation of transverse WBAM depending on the surface. Both groups had similar contributions from their legs. On the regular surface, the differences at the whole-body level came from reduced contributions from both the arms and the HTP segments in the PD group. On the irregular surface, the PD group increased their HTP angular momentum to the point it was no longer distinguishable from the HC group. Transverse WBAM generally reduces (Chiovetto et al., 2018; Thielemans et al., 2014) as a strategy to optimize alignment of the body during gait and minimize chances of crossover steps (Kent et al., 2019). However, in the present study we observed increases on the irregular surface in both groups. These increases indicate that arms are primarily used to cancel out angular momentum generated by the legs (Herr and Popovic, 2008) and are not necessarily actively utilized in the transverse plane as any safety strategy. Additionally, consequences of altered arm angular momentum are minimal, with implications primarily in metabolic cost associated with reduced arm swing (Ortega et al., 2008).

For the second objective, we hypothesized that within each health group, there would only be significant differences at the segmental level when comparing the regular to the irregular surface. This hypothesis was rejected for the sagittal plane for both groups and the transverse plane for the HC group. Small differences were identified in the sagittal and transverse planes in the HC group and not all the segment groups contributed to those significant differences. The differences observed in the HC group near the beginning of the trial (Fig. 4A) were not repeated

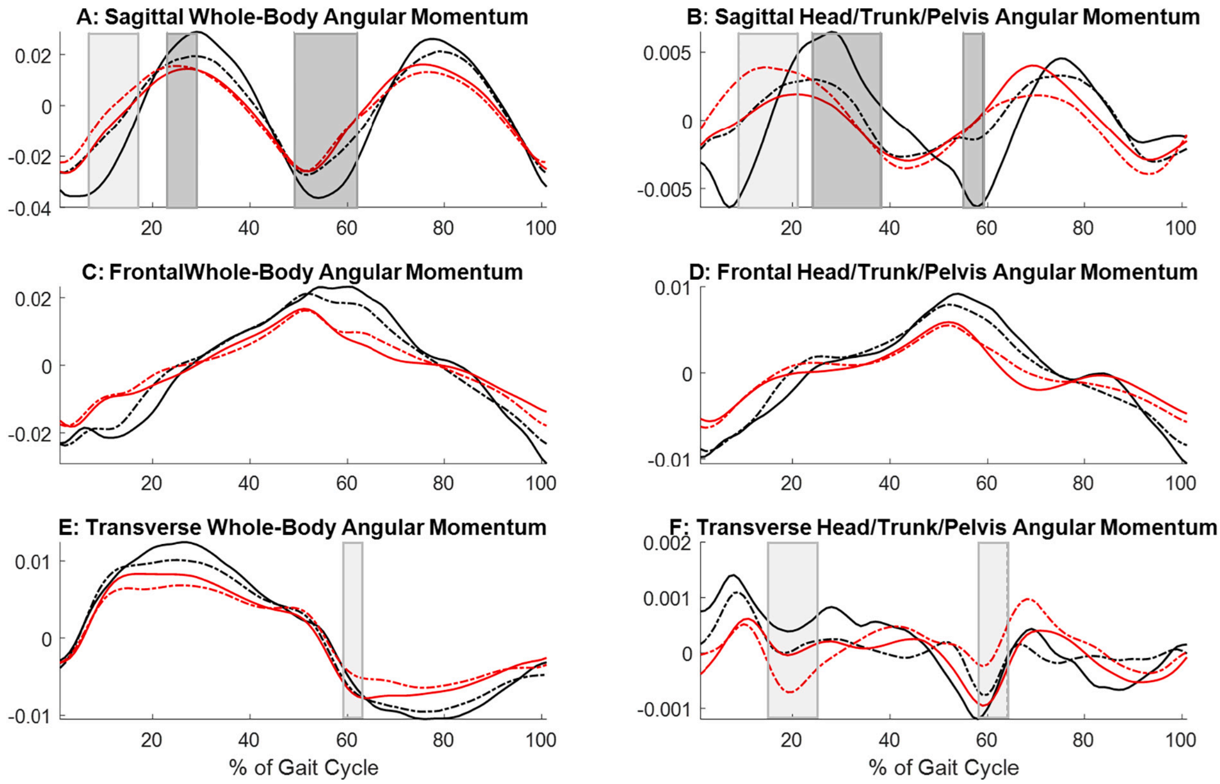

Fig. 4. Results for the npSPM paired *t*-tests for the whole-body angular momentum and head/trunk/pelvis segment about each principal axis. Dark shaded regions indicate significant ($p < 0.05$) difference between the irregular condition (solid black line) and the regular condition (dashed black line) for the PD group (black). Light shaded regions indicate significant ($p < 0.05$) difference between the irregular condition (solid red line) and the regular condition (dashed red line) for the HC group (red). All lines represent mean values for the groups and surface conditions. (For interpretation of the references to colour in this figure legend, the reader is referred to the web version of this article.)

following the second step of the gait cycle as would be expected if those differences were to be consistent. These findings align with prior research investigating healthy individuals on an irregular terrain that found significant but inconsistent changes to sagittal WBAM (Kent et al., 2019). We attribute this lack of consistency to the variability introduced by the irregular surface, and the general ability of the HC group to better regulate their WBAM depending on environmental demands (Martelli et al., 2013; Neptune and McGowan, 2011; Silverman et al., 2014). The changes in sagittal WBAM (Fig. 4A) for the HC group were the result of contributions from the HTP segment (Fig. 4B) and the legs (Fig. 5B). In the transverse plane, the changes in transverse WBAM (Fig. 4E) for the HC group were the result of increases in HTP angular momentum (Fig. 4F) that was not entirely cancelled out by the arms (Fig. 5E), which showed a reduction following the second heel strike of the GC. This is a somewhat surprising finding as the legs and arms are generally the greatest contributors to transverse angular momentum since they primarily cancel each other out (Herr and Popovic, 2008). The contribution of the HTP in this context indicates a strategy of increased torso rotation with corresponding arm swing without changes to stride length. For the PD group, our first hypothesis was only supported in the sagittal plane. Increases in sagittal WBAM (Fig. 4A) on the irregular surface were the result of increased contributions from the HTP segment (Fig. 4B), arms (Fig. 5A) and legs (Fig. 5B). Persons with PD usually present with reduced arm swing (Nieuwboer et al., 1998) so we had initially thought that the PD group would have reduced transverse angular momentum. However, recent research investigating arm swing (Gomez et al., Unpublished Data) identified that in the presence of an irregular terrain, persons with PD can increase their arm swing magnitude, which the present study shows is adequate for adding to control of WBAM.

This study identified important findings, but some limitations should be mentioned. Both group sizes were relatively small and thus failed the normality test; therefore, making generalizations to larger populations is difficult. Data for the HC group were also inconsistent from heel strike to heel strike. Though we allowed participants to acclimate to the two surfaces, prior work (Kent et al., 2019) suggests that there may be time-dependent changes to angular momentum regulation when ambulating on a challenging surface. This study was further limited by the choice to normalize WBAM using walking velocity. Though this is the technique most used in the literature (Herr and Popovic, 2008; Silverman et al., 2012; Martelli et al., 2013; Nolasco et al., 2019; Nazifi et al., 2020), it should be noted that due to the cross product in Eq.1, sagittal walking velocity does not contribute to the frontal plane angular momentum. Normalizing frontal plane angular momentum by disparate walking velocities can artificially skew the magnitude of the results. Future work should investigate the variance in steady-state gait on the irregular terrain over several gait cycles to better understand whether the results we found for the HC group between surfaces were an anomaly or characteristic of a gait variance that cannot be captured with a single gait cycle. Sensitivity analyses should also be performed investigating different normalization techniques utilized in the calculation and comparison of WBAM. Clinically, techniques should be investigated to address angular momentum control in the PD group, whether that be through novel therapy training or external interventions such as exoskeletons to mitigate fall risk on irregular terrains.

5. Conclusion

Persons with PD and the HC group both exhibited changes in WBAM regulation in the sagittal plane when walking on the irregular surface compared to the regular surface. All segments of the body contributed to this difference in the PD group while the HC group only showed differences in the HTP and legs segments. On the irregular surface, the PD

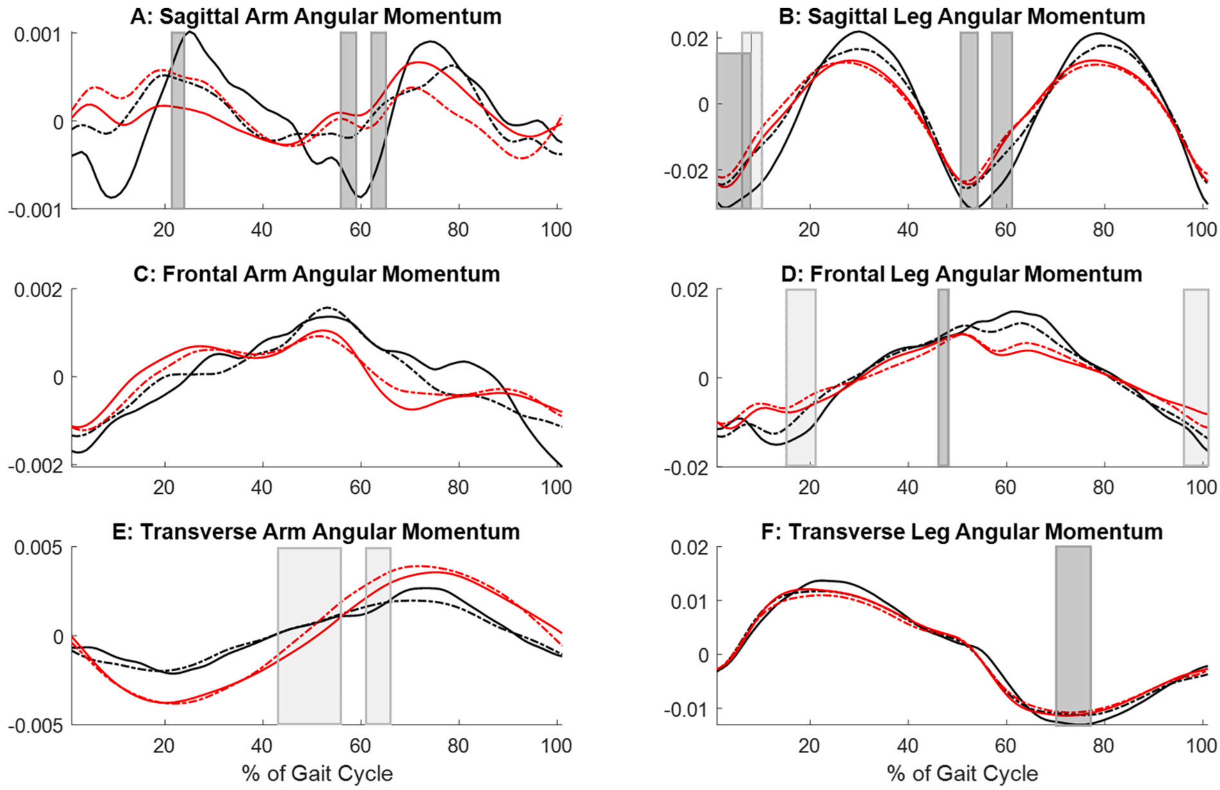

Fig. 5. Results for the npSPM paired t-tests for the angular momentum contributions from the arms and legs segments about each principal axis. Dark shaded regions indicate significant ($p < 0.05$) difference between the irregular condition (solid black line) and the regular condition (dashed black line) for the PD group (black). Light shaded regions indicate significant ($p < 0.05$) difference between the irregular condition (solid red line) and the regular condition (dashed red line) for the HC group (red). All lines represent mean values for the groups and surface conditions. (For interpretation of the references to colour in this figure legend, the reader is referred to the web version of this article.)

group exhibited both a magnitude and phase difference in whole-body and segmental angular momentum in the frontal and sagittal plane. These differences identify that the PD group is at a great risk of falling on an irregular terrain due to their delayed ability to regulate their angular momentum following heel strike. The most significant differences in regulation of angular momentum occurred during weight transfer. Though the PD group was able to increase the contributions of their arms to the regulation of whole-body angular momentum in the sagittal and frontal planes, the magnitude of their contribution was still small relative to the contributions of the legs and HTP segments. Consequently, therapies that target leg and torso control during weight transfer would provide the most benefit to persons with PD in order to reduce the risk of forward and lateral falls, especially on an irregular surface where health group differences were exacerbated.

Declaration of Competing Interest

Authors have no conflicts of interest to disclose.

Acknowledgements

This work was financially supported in part by grants from The National Science Foundation (NSF # 1162131) and the National Institute for Occupational Safety and Health Targeted Research Training Grant (NIOSH #5T42OH008414-16). All opinions, findings, and conclusions are exclusive to the author(s) and do not reflect the view and opinions of the NSF or NIOSH.

References

Begue, J., Peyrot, N., Dalleau, G., Caderby, T., 2019. Whole-body angular momentum during step initiation in young and older adults. Comput. Methods Biomech. Biomed. Eng. 22 https://doi.org/10.1080/10255842.2020.1714234.

Begue, J., Peyrot, N., Lesport, A., Turpin, N.A., Watier, B., Dalleau, G., et al., 2021. Segmental contribution to whole-body angular momentum during stepping in healthy young and old adults. Sci. Rep. 11 (1), 1–13. https://doi.org/10.1038/s41598-021-99519-y.

Benjamini, Y., Hochberg, Y., 1995. Controlling the false discovery rate: a practical and powerful approach to multiple testing. J. R. Stat. Soc. Ser. B Stat Methodol. 57 (1), 289–300. https://doi.org/10.1111/j.2517-6161.1995.tb02031.x.

Bennett, B.C., Russell, S.D., Sheth, P., Abel, M.F., 2010. Angular momentum of walking at different speeds. Hum. Mov. Sci. 29 (1), 114–124. https://doi.org/10.1016/j.humov.2009.07.011.

Brandon, S.C., Graham, R.B., Almosnino, S., Sadler, E.M., Stevenson, J.M., Deluzio, K.J., 2013. Interpreting principal components in biomechanics: representative extremes and single component reconstruction. J. Electromyogr. Kinesiol. 23 (6), 1304–1310. https://doi.org/10.1016/j.jelekin.2013.09.010.

Chester, V.L., Wrigley, A.T., 2008. The identification of age-related differences in kinetic gait parameters using principal component analysis. Clin. Biomech. 23 (2), 212–220. https://doi.org/10.1016/j.clinbiomech.2007.09.007.

Chiovetto, E., Huber, M.E., Sternad, D., Giese, M.A., 2018. Low-dimensional organization of angular momentum during walking on a narrow beam. Sci. Rep. 8 (1), 1–14. https://doi.org/10.1038/s41598-017-18142-y.

Gomez, N.G., Gubler, K.K., Foreman, K.B., Merryweather, A.S., 2020. Changes in step characteristics over a known outdoor surface transition: the effect of Parkinson disease. J. Appl. Biomech. 37 (1), 59–65. https://doi.org/10.1123/jab.2020-0124.

Hanavan Jr., E.P., 1964. A Mathematical Model of the Human Body. Air Force Aerospace Medical Research Lab Wright-Patterson AFB, OH.

Herr, H., Popovic, M., 2008. Angular momentum in human walking. J. Exp. Biol. 211 (4), 467–481. https://doi.org/10.1242/jeb.008573.

Jackson, J.E., 1991. A User's Guide to Principal Components. John Wiley & Sons Inc., New York.

Kent, J.A., Sommerfeld, J.H., Stergiou, N., 2019. Changes in human walking dynamics induced by uneven terrain are reduced with ongoing exposure, but a higher variability persists. Sci. Rep. 9 (1), 1–9. https://doi.org/10.1038/s41598-019-54050-z.

Li, W., Fey, N.P., 2021. Whole-body and segmental contributions to dynamic balance in stair ambulation are sensitive to early-stage Parkinson's disease. Engineering in

Medicine & Biology Society (EMBC). In: 43rd Annual International Conference of the IEEE, Curran Associates, Red Hook, NY, 2021, pp. 6441–6444. https://doi.org/10.1109/embc46164.2021.9630416.

Martelli, D., Monaco, V., Luciani, L.B., Micera, S., 2013. Angular momentum during unexpected multidirectional perturbations delivered while walking. IEEE Trans. Biomed. Eng. 60 (7), 1785–1795. https://doi.org/10.1109/tbme.2013.2241434.

Massano, J., Bhatia, K.P., 2012. Clinical approach to Parkinson's disease: features, diagnosis, and principles of management. Cold Spring Harb. Perspect. Med. 2 (6), a008870. https://doi.org/10.1101/cshperspect.a008870.

Monaghan, A.S., Huisinga, J.M., Peterson, D.S., 2021. The application of principal component analysis to characterize gait and its association with falls in multiple sclerosis. Sci. Rep. 11 (1), 1–10. https://doi.org/10.1038/s41598-021-92353-2.

Nazifi, M.M., Beschorner, K., Hur, P., 2020. Angular momentum regulation may dictate the slip severity in young adults. PLoS One 15 (3), e0230019. https://doi.org/10.1371/journal.pone.0230019.

Neptune, R.R., McGowan, C.P., 2011. Muscle contributions to whole-body sagittal plane angular momentum during walking. J. Biomech. 44 (1), 6–12. https://doi.org/10.1016/j.jbiomech.2010.08.015.

Neptune, R.R., McGowan, C.P., 2016. Muscle contributions to frontal plane angular momentum during walking. J. Biomech. 49, 2975–2981. https://doi.org/10.1016/j.jbiomech.2016.07.016.

Neptune, R.R., Vistamehr, A., 2019. Dynamic balance during human movement: Measurement and Control Mechanisms. J. Biomech. Eng. 141 (7) https://doi.org/10.1115/1.4042170.

Nieuwboer, A., Weerdt, W.D., Dom, R., Lesaffre, E., 1998. A frequency and correlation analysis of motor deficits in Parkinson patients. Disabil. Rehabil. 20 (4), 142–150. https://doi.org/10.3109/09638289809166074.

Nolasco, L.A., Silverman, A.K., Gates, D.H., 2019. Whole-body and segment angular momentum during 90-degree turns. Gait Posture 70, 12–19. https://doi.org/10.1016/j.gaitpost.2019.02.003.

Ortega, J.D., Fehlman, L.A., Farley, C.T., 2008. Effects of aging and arm swing on the metabolic cost of stability in human walking. J. Biomech. 41 (16), 3303–3308. https://doi.org/10.1016/j.jbiomech.2008.06.039.

Pataky, T.C., 2012. One-dimensional statistical parametric mapping in Python. Comput Methods Biomech Biomed Eng. 15 (3), 295–301. https://doi.org/10.1080/10255842.2010.527837.

Reid, S.M., Graham, R.B., Costigan, P.A., 2010. Differentiation of young and older adult stair climbing gait using principal component analysis. Gait Posture 31 (2), 197–203. https://doi.org/10.1016/j.gaitpost.2009.10.005.

T. Robert, B.C. Bennett, S.D Russell, C.A. Zirker, M.F. Abel. Angular momentum synergies during walking. Exp. Brain Res. 197(2) (2009) 185–197. doi:https://doi.org/10.1007/s00221-009-1904-4.

Silverman, A.K., Wilken, J.M., Sinitski, E.H., Neptune, R.R., 2012. Whole-body angular momentum in incline and decline walking. J. Biomech. 45 (6), 965–971. https://doi.org/10.1016/j.jbiomech.2012.01.012.

Silverman, A.K., Neptune, R.R., Sinitski, E.H., Wilken, J.M., 2014. Whole-body angular momentum during stair ascent and descent. Gait Posture 39 (4), 1109–1114. https://doi.org/10.1016/j.gaitpost.2014.01.025.

Stanhope, S.J., Kepple, T.M., McGuire, D.A., Roman, N.L., 1990. Kinematic-based technique for event time determination during gait. Med. Biol. Eng. Comput. 28 (4), 355–360. https://doi.org/10.1007/BF02446154.

Sutherland, D.H., et al., 1994. Kinematics of normal human walking. In: Rose, J., Gamble, J.G. (Eds.), Human Walking. Williams & Wilkins, p. 27.

Thielemans, V., Meyns, P., Bruijn, S.M., 2014. Is angular momentum in the horizontal plane during gait a controlled variable? Hum. Mov. Sci. 34, 205–216. https://doi.org/10.1016/j.humov.2014.03.003.

Tsuchida, W., Kobayashi, Y., Inoue, K., Horie, M., Yoshihara, K., Ooie, T., 2022. Kinematic characteristics during gait in frail older women identified by principal component analysis. Sci. Rep. 12 (1), 1–12. https://doi.org/10.1038/s41598-022-04801-2.

Vistamehr, A., Neptune, R.R., R. R., 2021. Differences in balance control between healthy younger and older adults during steady-state walking. J. Biomech. 128, 110717 https://doi.org/10.1016/j.jbiomech.2021.110717.

Winter, D.A., 1990. Kinetics: Force and movements of force, in: Biomechanics and Motor Control of Human Movement. Wiley, Hoboken, pp. 107–138.

Xu, H., Hunt, M., Foreman, K.B., Zhao, J., Merryweather, A.S., 2018. Gait alterations on irregular surface in people with Parkinson's disease. Clin. Biomech. 57, 93–98. https://doi.org/10.1016/j.clinbiomech.2018.06.013.